ACS OMEGA

http://pubs.acs.org/journal/acsodf

Article

Highly Selective and Sensitive Voltammetric Method for the Detection of Catechol in Tea and Water Samples Using Poly(gibberellic acid)-Modified Carbon Paste Electrode

Nambudumada S. Prinith, J. G. Manjunatha,* Abdullah A. Al-Kahtani, Ammar M. Tighezza, and Mika Sillanpää

Cite This: *ACS Omega* 2022, 7, 24679−24687

Read Online

ACCESS | Metrics & More | Article Recommendations

ABSTRACT: Despite the wide range of applications of catechol (CC) in agrochemical, petrochemical, textile, cosmetics, and pharmaceutical industries, its exposure to the environment leads to health issues as it is carcinogenic. This increased the concern over the risk of exposure level of CC in the environment, and monitoring its level has become critical. In this work, we report the fabrication of poly-gibberellic acid-modified carbon paste electrode (PGBAMCPE) to be a simple, viable, and effective electrochemical electrode for the determination of CC. This was synthesized by a simple electropolymerization method by the cyclic voltammetry (CV) technique. The electrodes were characterized by field emission electron microscopy, energy-dispersive X-ray spectroscopy, and electrochemical impedance spectroscopy. Compared to the bare carbon paste electrode, the sensitivity for CC fortified at PGBAMCPE in both CV and differential pulse voltammetry (DPV). We succeeded attaining a lower detection limit of 0.57 μM by the DPV method. The developed electrode was observed to be highly conductive, transducing, stable, and reproducible and was highly selective with anti-interfering properties from the determination of CC with hydroquinone simultaneously. The applicability of the electrode was confirmed from the detection CC in tea and water samples with good recoveries. This substantiates that PGBAMCPE is promising and consistent for the rapid monitoring of CC-contaminated area and clinical diagnosis.

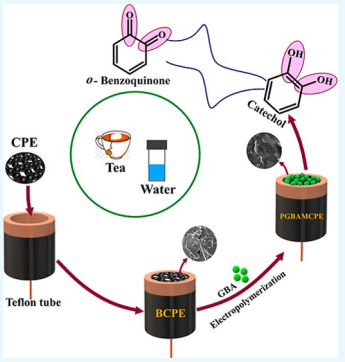

1. INTRODUCTION

Strict enforcement measures are necessary in regulating the exposure level of organic pollutants to prevent the risk of environmental and human health.[1−4] Therefore, there is a requisite to delve on the exposure level of these toxic wastes. The organic pollutants containing phenolic derivatives are the major threat to the environment. Such organic compounds arise from agrochemical, petroleum, textile, and pharmaceutical industries. Catechol (CC) (1,2-dihydroxy benzenediols) is one of the ortho-isomers of the three benzenediols. It is an acute toxic organic phenol compound, and on contact with human skin, it leads to eczematous dermatitis and is also carcinogenic.[5,6] CC is greatly produced due to anthropogenic activities like processing of coal tar, manufacturing of insecticides, production of perfumes and drugs, waste incineration plants, and so forth.[7] Small amounts of CC are predominantly found in naturally occurring plants like pine, tea, oak, and so forth and fruits and vegetables like apples, potatoes, onions, and so forth.[8] A larger dosage of CC affects the central nervous system. Therefore, there is an upsurge of importance in governing CC environmentally and clinically.

After going through various literature reports, the quantitative analysis of CC was carried out by utilizing innumerable sophisticated methods, such as HPLC, GC−mass spectrometry, flow injection chemiluminescence, fluorescence, and so forth,[9−12] which require expensive apparatus, pretreatments, trained personnel to handle and operate the apparatus, and is a time-consuming process.[13] Hence, the applications of the aforementioned methods were greatly prevented in the rapid detection of target analytes. In contrast to the approach of complicated methods, voltammetry has achieved more attention for its intrinsic merits of economical apparatus, sensitivity, simple and smooth operation, portability, and immediate on-site response of target analytes disclosing the charge-transfer abilities.[14−16] As CC is electrochemically active, its analytical reaction has been improvized by numerous newly developed modified electrochemical sensors. As a result, these studies support in understanding the electrochemical activity of the target analyte. Further, it helps in the quantification of trace amounts of target analytes present in the biological samples.

Received: April 24, 2022
Accepted: June 20, 2022
Published: June 30, 2022

https://doi.org/10.1021/acsomega.2c02553
ACS Omega 2022, 7, 24679−24687

Thus, voltammetric studies provide innumerable applications in monitoring the environment and in clinical diagnosis.

Carbon paste electrode (CPE) has provoked huge interest in the area of sensing materials. This is certainly due to the aspects of effortless preparation, biocompatibility, rapid surface regeneration, and easy modification with low Ohmic resistance. This sensing material can be improvized, focusing on the significant catalytic behavior, high conductivity, wider surface area as well as the sensitivity of the target analyte, by enhancing the oxidation peak current and lowering the oxidation potential.[17] Electropolymerization is a facile technique for the fabrication of surface-modified CPEs. Gibberellic acid is a water-soluble phytohormone, and there is no literature survey about its modification on the electrode, except one.[18] GA is a dihydroxy-acid enclosing a γ-lactone ring owing to a double bond at the terminal methylene group and a free −COOH group in its structure.[19] These functional groups are suitable for the modification of the electrode. The film was fabricated through the electropolymerization method, which provides good rewards compared to other deposition methods in relation to standardizing the thickness of the film, and holds higher stability, simple methodology, and is reasonable.

To the best of our knowledge, there were no reports regarding poly-gibberellic acid-modified carbon paste electrode (PGBAMCPE) for CC. This motivated us to fabricate PGB on a CPE film that assured sensitive determination of CC. In this context, we have effectively implemented a voltammetric electrode which is proficient in regulating a wide range of CC concentrations without any disturbance from hydroquinone (HQ). The developed electrode displayed beneficial characteristics along with simple fabrication and renewability of the surface, being an apt applicant for voltammetric quantification of real samples.

2. MATERIALS AND METHODS

2.1. Instrumentation. Every electrochemical measurement and electrochemical impedance study were recorded with CH instruments model CH-6038E (electrochemical workstation, USA). The pH of the buffer solution was measured by a digital Equiptronics apparatus with an electrode. Voltammetric measurements were carried out by utilizing the typical three-electrode system contained in a single compartment cell with the saturated calomel electrode as a reference electrode, platinum wire as an auxiliary electrode, and PGBAMCPE and bare CPE (BCPE), respectively. The data were secured in the desktop. FE-SEM and EDX data were obtained from DST-PURSE Laboratory, Mangalore University.

2.2. Chemicals. CC of 99%, HQ of 98%, sodium phosphate dibasic dihydrate of 99.5%, and sodium phosphate monobasic monohydrate of 99% were procured from Sisco Research Lab, India. GBA of 90%, graphite powder of 90%, KCl, NaOH, and silicone oil were bought from Nice Chemicals, India. Potassium ferrocyanide trihydrate $K_4[Fe(CN)_6]\cdot 3H_2O$ of 98.5% was procured from Himedia, India. Here, the chemicals used were of analytical grade and without additional refinement.

2.3. Preparation of Stock Reagents. The stock solutions of 25×10^{-4} M CC, 25×10^{-3} M GBA, 25 mM $K_4[Fe(CN)_6]$, and 0.1 M KCl were prepared by dissolving these reagents in deionized water. 0.1 M of phosphate-buffered saline (PBS) was prepared by dissolving the required amounts of 0.1 M sodium phosphate dibasic dihydrate and 0.1 M sodium phosphate monobasic monohydrate in adequate volume of distilled water.

2.4. Fabrication of Unmodified as well as Modified Electrode. The percentage proportion of graphite powder and silicone oil was optimized to 70:30. The mixture of these two compounds was perfectly blended with the support of the pestle in an agate mortar for 1 h. From this, a cohesive paste was obtained. A bit of the prepared cohesive paste was sealed gently into the hollow space of the Teflon tube with an internal diameter of 3 mm, which functions as a sensing body. Further, it was smoothened to attain an even surface. The obtained surface was cleaned with double distilled water. However, the other end of the tube was associated to the external circuit via a copper wire. Polymeric GBA thin films were tailored smoothly by the cyclic voltammetry (CV) method. The growth of the polymer was optimized by a number of deposition cycles. As soon as continuous running of 15 CV cycles at the potential range of −1.5 to 1.5 V, the electrode was cleaned with double distilled water to remove the leftover GBA monomers.

2.5. Preparation of Real Samples. About 1 g of tea powder was weighed and boiled in 25 mL of distilled water and then cooled. The above sample was centrifuged for half an hour. The collected supernatant was diluted with normal pH PBS. Without any pretreatment, tap water samples were diluted with PBS in the ratio of 1:5.

3. RESULTS AND DISCUSSION

3.1. Fabrication and Optimization of PGBAMCPE for CC Determination. 1 mM solution of GBA was polymerized electrochemically in 0.1 M PBS containing 0.1 M NaH_2PO_4 and 0.1 M Na_2HPO_4, at pH 6.5. Poly(gibberellic acid) (PGBA) thin films were encrusted on BCPE by performing 20 sweep potential cycles successively within the range of −400 mV to 1000 mV, sweeping at a scan rate of 50 mV s^{-1}.

The performance of PGBA films can be improved for the electrocatalytic activity of CC by optimizing the number of sweep potential cycles. From Figure 1 it is observed that there

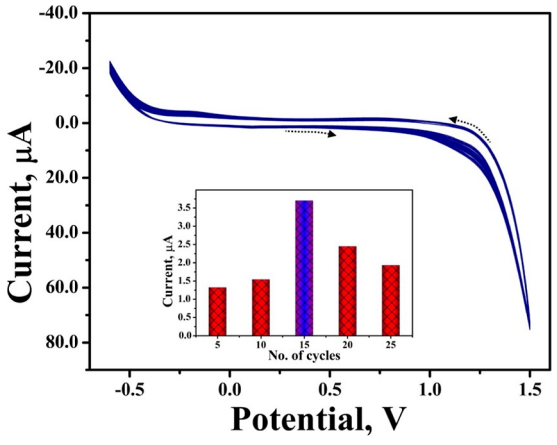

Figure 1. CVs recorded for the fabrication of PGBAMCPE using 1 mM of GBA in 6.5 pH of 0.1 M PBS at a scan rate 0.05 Vs^{-1} for 15 cycles repeatedly. Inset: optimization of PGBA cycles of electropolymerization.

was a gradual increase in the sensitivity response with the increase in the number of sweep potential cycles of MB, and beyond 15 cycles, the sensitivity was drastically dropped because of the saturation on the film which is responsible for resisting the electron transfer. Moreover, this suggests that the thickness of the film beyond a certain limit creates no active

https://doi.org/10.1021/acsomega.2c02553
ACS Omega 2022, 7, 24679−24687

surface area. Thus, 15 potential cycles were chosen for the studies here.

3.2. Characterization of the Surface of BCPE and PGBAMCPE. Figure 2 shows the FE-SEM and EDX mapping

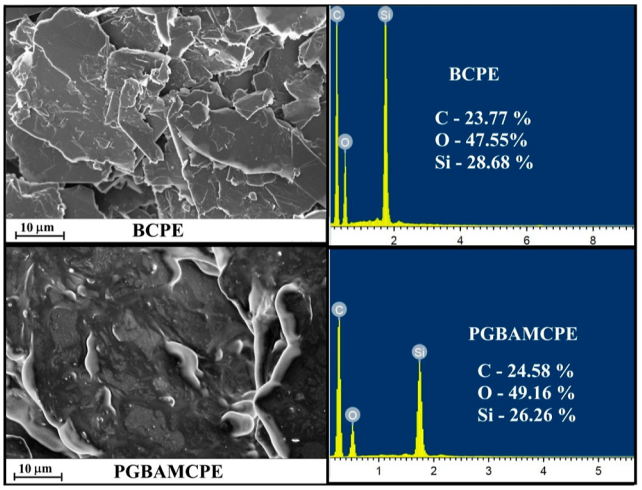

Figure 2. Characterization of BCPE and PGBAMCPE by FE-SEM and EDX.

images of both BCPE and PGBAMCPE. To examine the surface morphology, we employed FE-SEM. As in the figure, BCPE displayed a distinctive flaky asymmetrical shape with roughness. However, in PGBAMCPE, the uniform film without any roughness was covered on the flaky structure. This substantiates that the thin layer of PGBA was incorporated in BCPE. In both the electrodes, EDX mapping for carbon [C], oxygen [O], and silicone (Si) was done. The percentage composition of C and O in PGBAMCPE was higher compared to that in BCPE. This authenticates that the surface was successfully modified.

3.3. Electrochemical and Impedance Characterization of PGBAMCPE and BCPE. Cyclic voltammogram of 1 mM of $K_4[Fe(CN)_6]$ in the supporting electrolyte 0.1 M KCl presented an increase in the redox peak current for PGBAMCPE than BCPE in Figure 3a. This shows that the electrocatalytic activity has been successfully enhanced at the surface of the modified electrode.

In this reversible process, we calculated the electroactive surface area by using the Randle−Sevcik equation[20]

$$I_p = (2.65 \times 10^5) n^{3/2} A D^{1/2} \nu^{1/2} C \quad (1)$$

where I_p is the anodic peak current in amperes attained for $K_4[Fe(CN)_6]$, n is the number of electrons involved in the reversible process, A is the electroactive surface area in cm^2, D is the diffusion coefficient in $cm^2\ s^{-1}$, C is the concentration of $K_4[Fe(CN)_6]$ in mol cm^{-3}, and ν is the scan rate in V s^{-1}.

PGBAMCPE exhibited a larger electroactive surface area of 0.79 cm^2 which is responsible for the increase of redox peaks compared to that of BCPE of 0.39 cm^2.

To the above solution, electrochemical impedance spectroscopy (EIS) characterization was also carried out. The attained Nyquist plot for the duo electrodes is displayed in Figure 3b. This plot fitted well with an equivalent circuit owing to the parameters such as CPE—constant phase element conductance, C_1−−outer capacitance, C_2−−inner capacitance, R_1—outer resistance, R_2, R_3—inner resistance, R_s—resistance of the electrolyte solution, W—Warburg impedance, and R_{ct}—resistance of charge transfer at the electrode, respectively. BCPE and PGBAMCPE displayed two frequency sections. It is observed in the Figure 3b that BCPE displayed a long straight line owing to the higher range of frequency with low capacitance and greater R_{ct} value of 356.1 Ω. However, PGBAMCPE showed a shorter line owing to the lower frequency range with high capacitance and lower R_{ct} value of 185.7 Ω. This proves that the surface modified with PGBA tends to be highly conductive, and the increase in electroactive surface area resulted in efficient electrocatalytic activity.

3.4. Impact of Supporting Electrolyte on CC. The electrochemical redox behavior of CC was studied over the range of pH of 6.0 to 8.0 at the scan rate of 0.05 V s^{-1}. As CC has two hydroxyl groups, it is necessary to examine the pH on the structure of CC at PGBAMCPE. As it is seen in Figure 4a, as the pH increases steadily, the anodic peak potential shifts steadily to the negative potential. This substantiates that the elimination of electrons from CC induces the loss of protons, as in Scheme 1.[21] Another observation from Figure 4b is that the anodic peak increases from pH 6.0 to 7.0, and beyond 7, the pH decreases. Therefore, the best supporting electrolyte for the electrochemical redox behavior of CC was chosen at neutral pH 7.0 of 0.1 M PBS. At higher alkalinity, there is another diminished redox peak which shows that there is a

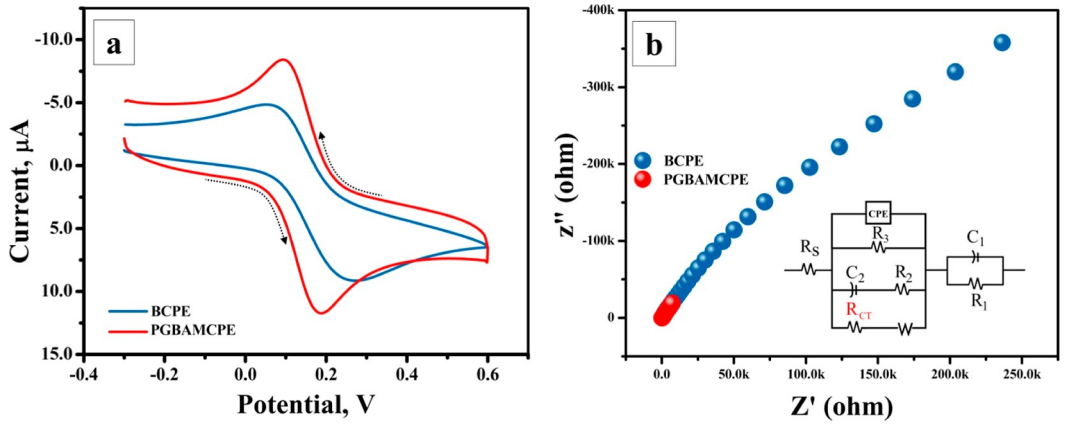

Figure 3. (a). CV behavior of 1 mM of $K_4[Fe(CN)_6]$ with 0.1 M KCl (scan rate 0.1 V s^{-1}) at BCPE and PGBAMCPE. (b). Nyquist curves for BCPE and PGBAMCPE with the fitted Randles circuit for characterizing EIS data.

https://doi.org/10.1021/acsomega.2c02553
ACS Omega 2022, 7, 24679−24687

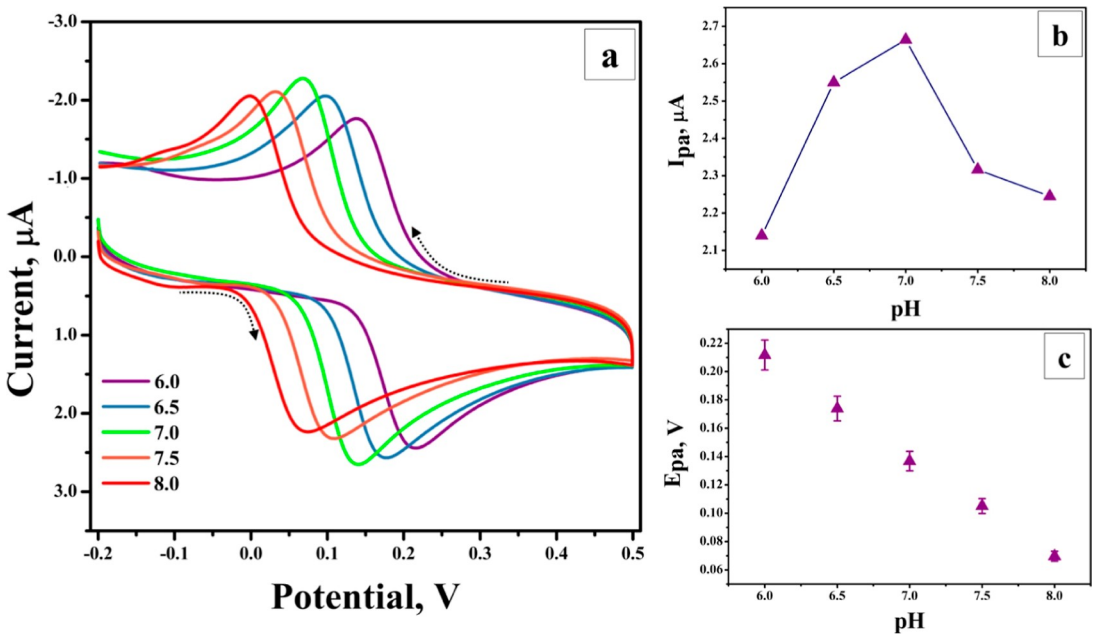

Figure 4. (a). CV curves of CC in 0.1 M PBS of varying pH (6.0−8.0) with 0.05 V s^{-1} scan rate at PGBAMCPE. (b). Variation of oxidative peak current with pH of 0.1 M PBS. (c). Impact of pH (0.1 M PBS) on the CC oxidation peak potential.

Scheme 1. Redox Mechanism of CC

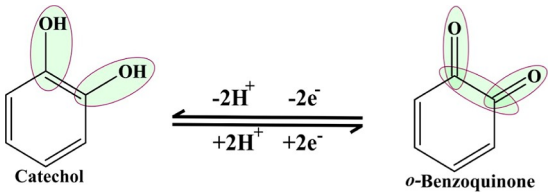

chance of hydroxyl group reacting to *o*-benzoquinone to form 2-hydroxy quinone or semiquinone.[22] From the potential−pH plot in Figure 4c, the linear regression (LR) equation obtained was E_{pa} (V) = 0.6 (V) − 0.068 pH; from this, the slope obtained was 68 mV/pH which is relatively closer to the Nernstian value of 59 mV/pH. This substantiates that the electrons and protons engaged are of equal ratio.

3.5. Impact of Scan Rate on CC Peak. Figure 5a illustrates the voltammogram recorded for 0.1 mM of CC with neutral pH from the oxidative direction of −0.2 to +0.5 and reversed to −0.2 at variable sweep rates (0.025 to 0.25 V s^{-1}). One more observation is that the CC peak potential slightly shifts to be positive, with the increase of the sweep rate. Figure 5b exhibits linearity among the peak current and square root of the scan rate with the obtained LR equation of I_{pa} (A) = 7.74 × 10^{-8} + 1.12 ×10^{-5} $\nu^{1/2}$ (R^2 = 0.998) and I_{pc} = 2.44 × 10^{-7} − 1.2 × 10^{-5} $\nu^{1/2}$ (R^2 = 0.9998). This means that the redox process of CC at PGBAMCPE is diffusion-controlled. Again, to confirm this, the plot of log I_{pa} versus log ν (Figure 5c) was displayed with linearity with the LR equation of log I_{pa} = −4.9 + 0.49 log ν. The slope 0.49 is nearer to 0.5, confirming that the reaction was diffusion-controlled at the superficial layer of the electrode.[23−28]

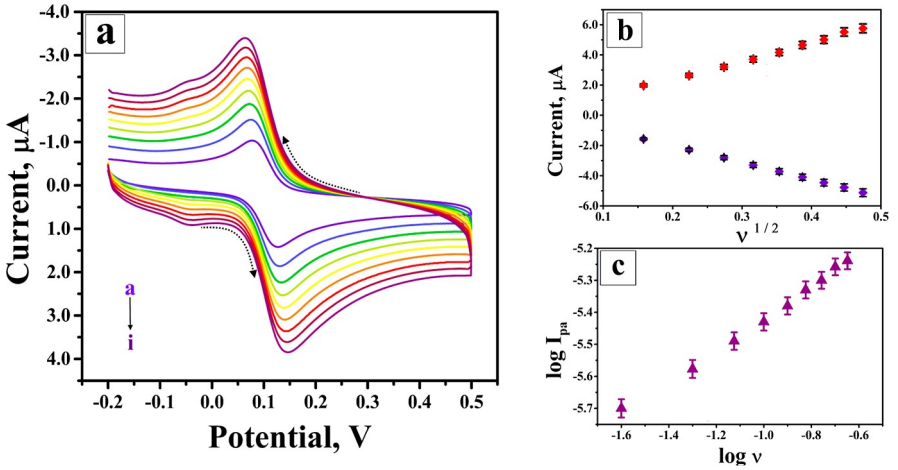

Figure 5. (a). CV curves of CC in 0.1 M PBS of pH 7.0 of varying scan rates [0.025 (a)−0.225 (i)] V s^{-1} at PGBAMCPE. (b). Variation of anodic and cathodic peak currents with the square root of the scan rate. (c). Linear dependence of log I_{pa} on log ν.

https://doi.org/10.1021/acsomega.2c02553
ACS Omega 2022, 7, 24679−24687

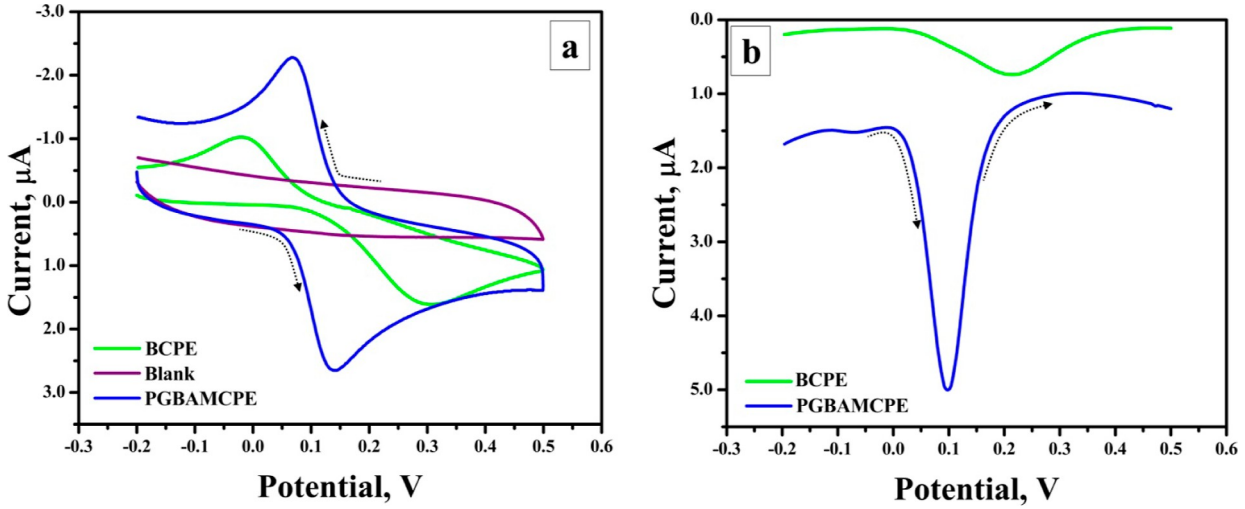

Figure 6. Response of CC with pH 7 of 0.1 M PBS at BCPE and PGBAMCPE by (a) CV (0.05 V s^{-1}) and (b) DPV.

3.6. Voltammetric Response of CC at BCPE and PGBAMCPE. Voltammetric response was examined for 0.1 mM of CC at 7.0 PBS at 0.05 V s^{-1} by means of CV and differential pulse voltammetry experiments. The cyclic voltammograms were demonstrated to show both oxidation and reduction processes for CC at BCPE and PGBAMCPE, as depicted in Figure 6a. In the case of BCPE, two broader peaks are observed with a change in the peak potential of 274.7 mV, which is greater than 59 mV, and the ratio of the peak current is 1.6, authenticating the quasi-reversible process. However, PGBAMCPE portrayed pronounced redox peaks with the change in the peak potential of 64.5 mV almost closer to 59 mV, and the ratio of the peak current was 1.2, almost equal to unity, authenticating the reversible process. The inflation of the redox peaks of CC was observed at PGBAMCPE than BCPE. In addition to this, there was no single peak, except that the background current was observed for the absence of the CC analyte at PGBAMCPE as recognized as blank in Figure 6a. In differential pulse voltammetry (DPV), as it is highly sensitive than CV, the anodic peak current observed for CC at PGBAMCPE was 5 μA, whereas in CV, it was 0.137 μA. The same trend was observed in CV hereto; the peak was fivefold greater with a lower potential at PGBAMCPE compared to BCPE. Moreover, at PGBAMCPE, the CC anodic peak was observed at the reduced activation energy of 11 mV compared to BCPE, as depicted in Figure 6b. The inflated peak with a rapid electron transfer of CC was enhanced at PGBAMCPE as a result of higher surface area.[29−31] The probable mechanism of CC on PGBAMCPE is depicted in Scheme 2.

3.7. DPV Method for the Quantification of CC. To enhance the detection limit (DL) of CC, we utilized the highly sensitive DPV method at PGBAMCPE. Under optimized circumstances, Figure 7a represents the DP voltammograms of the variable concentration of CC. CC oxidation occurred at the same potential of 0.098 V for variable concentration over the range of 2−100 μM. Another observation from Figure 7a was that the anodic peak currents inflated linearly with the increase of concentration. Figure 7b represents the relationship between the oxidative peak current responses and variable concentrations of CC. Here, it is witnessed with two linear dynamic ranges. The LR equation obtained for 2−10 μM is I_{pa} (μA) = 0.685 μA + 0.0327 C (M) [R^2 = 0.997] and that for

Scheme 2. Schematic Representation of the Probable Mechanism of CC on PGBAMCPE

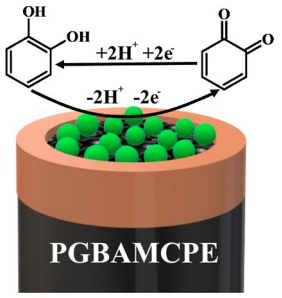

10−100 μM is I_{pa} (μA) = 0.789 μA + 0.0173 C (M) [R^2 = 0.998]. The reason for two linear ranges was plausibly due to the kinetic limitations of the reaction toward the surface of the electrode in the mode of diffusion. The DL and quantification limit (QL) were measured to be 0.57 μM (3S/N) and 1.9 μM (10S/N), respectively, where "S" is the standard deviation of blank for five replicates and "N" is the slope of the calibration plot.[32] It is worthy to report that compared to the other reported literature works, we have achieved lower DL in this work for the quantification of CC at neutral pH. Table 1 portrays the relative study of PGBAMCPE with published literature reports. From the results derived from the tabulated reports, we conclude that PGBAMCPE exhibits good sensitivity.

3.8. Selectivity Study of CC along with HQ by DPV. Like CC, HQ (1,4-dihydroxy benzenediol) is also another type of structural isomer of benzenediols, where the hydroxyl group is at the para-position, having the same molecular weight. Hence, both these frequently coexist in the environment.[50] However, it is tedious to determine them simultaneously as they mutually interfere. Based on this, we inspect the simultaneous determination of CC and HQ. Figure 8 displays the DP voltammograms of CC and HQ at PGBAMCPE, revealing pronounced peaks for both. When the concentration of CC was varied and the concentration of HQ was kept constant (Figure 8a),it was observed that the peak of CC ascended with the increase of CC concentration, but the HQ peak almost remained at the same position. In Figure 8b, the concentration of CC was kept constant and the HQ

https://doi.org/10.1021/acsomega.2c02553
ACS Omega 2022, 7, 24679−24687

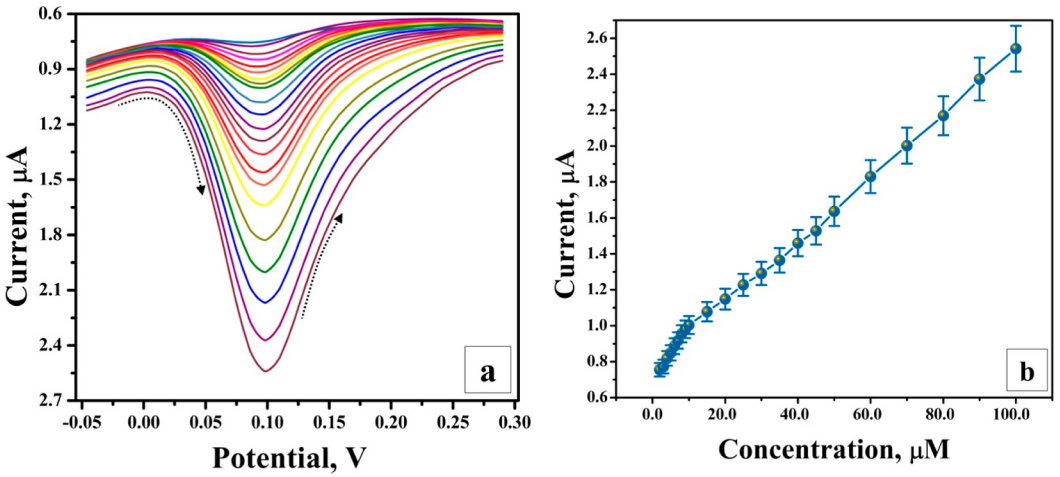

Figure 7. (a) DPVs of the concentration variation of CC in 7.0 PBS at PGBAMCPE. (b) Calibration plot.

Table 1. PGBAMCPE Characteristics Compared with Other Reported Electrodes

sl. no.	name of the electrodes	mode	linear range (μM)	detection limit (μM)	reference
1	silsesquioxane-MCPE	DPV	10−300	10.0	33
2	Cu(Sal-β-Ala)(3,5-DMPz)2]/SWCNTs/GCE	DPV	5−215	3.5	34
3	SDBS/GCE	DPV	3.0−400	3.0	35
4	MWCNT-NF-PMG/GCE	DPV	400−1300	2.5	36
5	RGO-MWNTs	DPV	5.5−540	1.8	37
6	PEDOT/GO/GCE	DPV	2−400	1.6	38
7	LDHf/GCE	DPV	3.0−1500	1.2	39
8	laccase-cysteine/cysteine/gold SPE	Chronoamperometry	20−2400	1.2	40
9	PASA/MWNTs/GCE	DPV	6.0−700	1.0	41
10	poly(proline)MGPE	CV	2−45	0.87	42
11	poly(rosaniline)MGPE	DPV	2.0−100	0.82	43
12	Au−PdNF/rGO/GCE	DPV	2.5−100	0.8	44
13	LRG/GCE	DPV	2−300	0.8	45
14	TRGO/GCE	DPV	1−500	0.8	46
15	graphene-doped CILE	DPV	10−300	0.74	47
16	poly(phenylalanine)/GCE	DPV	10−140	0.7	48
17	MIL-101 (Fe) MCPE	DPV	2−100	0.62	49
18	MWCNT-modified GCE	LSV	2−100	0.6	49
19	PGBAMCPE	DPV	2−10	0.57	present work

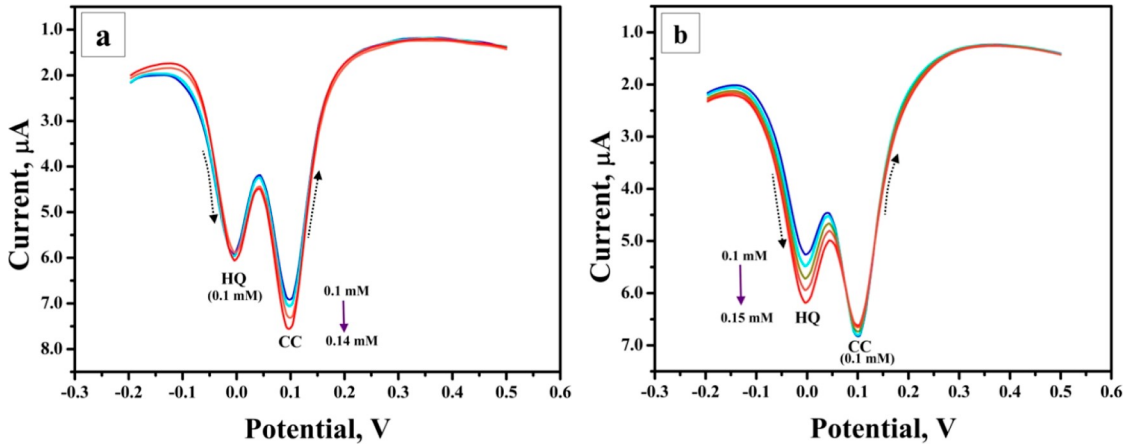

Figure 8. (a). DPVs with the change in the concentration (0.1−0.14 mM) of CC and 0.1 mM of HQ in PBS 7.0 (b). DPVs of 0.1 mM CC and change in the concentration (0.1−0.14 mM) of HQ in PBS 7.0.

concentration varied. As the HQ concentration varied, the peak current also gradually increased, and there was a slight decrease of peak in CC which almost remained constant without disturbing the potential shift. This substantiates that PGBAMCPE is highly selective and specific with anti-interfering characteristics.

https://doi.org/10.1021/acsomega.2c02553
ACS Omega 2022, 7, 24679−24687

3.9. Reproducibility, Repeatability, and Stability. Reproducibility of PGBAMCPEs was examined in five consecutive CC determinations by utilizing the CV method. The relative standard deviation (RSD) was calculated to be 1.57%, illustrating the proposed electrodes to have admirable reproducibility. Then, to examine the repeatability, five trials of CC solution at the same PGBAMCPE by CV were done. The RSD was measured to be 2.1%. At last, to check the electrode's long-term stability, PGBAMCPE was stored in a desiccator for 1 week. The peak current of CC after storage was retained to be 93.02%. This result displays PGBAMCPE to have good long-term steadiness.

3.10. Practical Application of PGBAMCPE. PGBAMCPE was applied for quantifying CC in the following real samples, that is, tea and tap water. The standard addition method was employed by spiking CC of three different concentrations into the real samples. For each concentration, three trial measurements were carried out for both the samples. We achieved good recovery percentage, as illustrated in Table 2. This authenticates the ability of PGBAMCPE for determining CC in real samples.

Table 2. Recovery Report of CC at PGBAMCPE in Two Different Real Samples

sample	added (μM)	found (μM)	recovery %
tea sample	6	5.77	96.2
	7	6.8	97.2
	8	7.71	96.4
tap water	6	5.73	95
	7	6.75	96.5
	8	7.7	96.3

4. CONCLUSIONS

Phenolic derivatives are the major organic pollutants, and their exposure is responsible for environmental pollution. Therefore, in an attempt to monitor the exposure of CC level in the environment, we have developed an electrochemical sensor for the analysis of CC in an economical way. PGBAMCPE was the outcome after the electropolymerization of gibberellic acid on BCPE through CV. This experimental work authenticates the voltammetric response of CC under optimized conditions to PGBAMCPE, and its detection in real sample analysis was succeeded. The intense electrocatalytic effect with rapid electron-transporting ability was attained at PGBAMCPE for CC determination. PGBAMCPE was significant with high sensitivity with DL of 0.57 μM which is adequate to monitor CC in various samples. It was succeeded to be highly selective in determining simultaneously with HQ with two well-defined peaks. PGBAMCPE was highly stable with good reproducibility. This confirms that PGBAMCPE is capable enough for CC quantification.

AUTHOR INFORMATION

Corresponding Author

J. G. Manjunatha − *Department of Chemistry, FMKMC College, Constituent College of Mangalore University, Madikeri 571201 Karnataka, India;* orcid.org/0000-0002-0393-2474; Email: manju1853@gmail.com

Authors

Nambudumada S. Prinith − *Department of Chemistry, FMKMC College, Constituent College of Mangalore University, Madikeri 571201 Karnataka, India*

Abdullah A. Al-Kahtani − *Chemistry Department King Saud University, Riyadh 11451, Saudi Arabia*

Ammar M. Tighezza − *Chemistry Department King Saud University, Riyadh 11451, Saudi Arabia*

Mika Sillanpää − *Chemistry Department, College of Science and Chemical Engineering, Aarhus University, Aarhus C 8000, Denmark*

Complete contact information is available at: https://pubs.acs.org/10.1021/acsomega.2c02553

Author Contributions

N.S.P: experimentation, preparation of the draft, visualization, and editing. J.G.M: supervision, review, and visualization. A.A.A.-K.: visualization. A.M.T.: visualization. M.S.: visualization.

Notes

The authors declare no competing financial interest.

ACKNOWLEDGMENTS

N.S. Prinith immensely acknowledge the financial support by KSTEPS, DST, Govt. of Karnataka fellowship (CHE-06: 2019−20). A.M.T. and A.A.A.-K. are grateful to the researchers supporting project number (RSP-2021/266), King Saud University, Riyadh, Saudi Arabia.

REFERENCES

(1) Hojjati-Najafabadi, A.; Mansoorianfar, M.; Liang, T.; Shahin, K.; Karimi-Maleh, H. A review on magnetic sensors for monitoring of hazardous pollutants in water resources. *Sci. Total Environ.* **2022**, *824*, 153844.

(2) Karimi-Maleh, H.; Darabi, R.; Shabani-Nooshabadi, M.; Baghayeri, M.; Karimi, F.; Rouhi, J.; Alizadeh, M.; Karaman, O.; Vasseghian, Y.; Karaman, C. Determination of D& C Red 33 and Patent Blue V Azo dyes using an impressive electrochemical sensor based on carbon paste electrode modified with ZIF-8/g-C3N4/Co and ionic liquid in mouthwash and toothpaste as real samples. *Food Chem. Toxicol.* **2022**, *162*, 112907.

(3) Buledi, J. A.; Mahar, N.; Mallah, A.; Solangi, A. R.; Palabiyik, I. M.; Qambrani, N.; Karimi, F.; Vasseghian, Y.; Karimi-Maleh, H. Electrochemical quantification of mancozeb through tungsten oxide/reduced graphene oxide nanocomposite: A potential method for environmental remediation. *Food Chem. Toxicol.* **2022**, *161*, 112843.

(4) Karimi-Maleh, H.; Beitollahi, H.; Senthil Kumar, P.; Tajik, S.; Mohammadzadeh Jahani, P.; Karimi, F.; Karaman, C.; Vasseghian, Y.; Baghayeri, M.; Rouhi, J.; Show, P. L.; Rajendran, S.; Fu, L.; Zare, N. Recent advances in carbon nanomaterials-based electrochemical sensors for food azo dyes detection. *Food Chem. Toxicol.* **2022**, *164*, 112961.

(5) Kim, K. Influences of environmental chemicals on atopic dermatitis. *Toxicol. Res.* **2015**, *31*, 89−96.

(6) McCue, J. M.; Link, K. L.; Eaton, S. S.; Freed, B. M. Exposure to Cigarette Tar Inhibits Ribonucleotide Reductase and Blocks Lymphocyte Proliferation. *J. Immunol.* **2000**, *165*, 6771−6775.

(7) Liu, Q.; Zou, L.; Sun, Q.; Li, X.; Chen, Y. Enzyme and Microbial Technology A voltammetry biosensor based on self-assembled layers of a heteroleptic tris (phthalocyaninato) europium triple-decker complex and tyrosinase for catechol detection. *Enzyme Microb. Technol.* **2020**, *139*, 109578.

(8) Zhou, L.; Shan, X.; Jiang, D.; Wang, W.; Chen, Z. Electrochemical luminescence sensor based on CDs @ HKUST-1

composite for detection of catechol. *J. Electroanal. Chem.* **2020**, *871*, 114215.
(9) Cui, H.; He, C.; Zhao, G. Determination of polyphenols by high-performance liquid chromatography with inhibited chemiluminescence detection. *J. Chromatogr. A* **1999**, *855*, 171−179.
(10) Hofer, I.; Gautier, L.; Sauteur, E. C.; Dobler, M.; Python, A.; O'Reilly, C.; Gisi, D.; Tinguely, E.; Wehren, L.; Fidalgo, E. G. A Screening Method by Gas Chromatography-Mass Spectrometry for the Quantification of 24 Aerosol Constituents from Heat-Not-Burn Tobacco Products. *Beitrage zur Tab. Int. Contrib. to Tob. Res.* **2019**, *28*, 317−328.
(11) Zhao, L.; Lv, B.; Yuan, H.; Zhou, Z.; Xiao, D. A Sensitive Chemiluminescence Method for Determination of Hydroquinone and Catechol. *Sensors* **2007**, *7*, 578−588.
(12) Lin, Z.-Y.; Kuo, Y.-C.; Chang, C.-J.; Lin, Y.-S.; Chiu, T.-C.; Hu, C.-C. Highly sensitive sensing of hydroquinone and catechol based on β-cyclodextrin-modified carbon dots. *RSC Adv.* **2018**, *8*, 19381−19388.
(13) Manjunatha, J. G.; Raril, C.; Prinith, N. S.; Pushpanjali, P. A.; Charithra, M. M.; Tigari, G.; Hareesha, N.; D'Souza, E. S.; Amrutha, B. M. Fabrication, characterization and application of poly-(acriflavine) modified carbon nanotube paste electrode for the electrochemical determination of catechol. *Handbook of Nanomaterials for Sensing Applications* **2021**, *10*, 105−117.
(14) Cheraghi, S.; Taher, M. A.; Karimi-Maleh, H.; Karimi, F.; Shabani-Nooshabadi, M.; Alizadeh, M.; Al-Othman, A.; Erk, N.; Yegya Raman, P. K.; Karaman, C. Novel enzymatic graphene oxide based biosensor for the detection of glutathione in biological body fluids. *Chemosphere* **2022**, *287*, 132187.
(15) Karimi-Maleh, H.; Arotiba, O. A. Simultaneous determination of cholesterol, ascorbic acid and uric acid as three essential biological compounds at a carbon paste electrode modified with copper oxide decorated reduced graphene oxide nanocomposite and ionic liquid. *J. Colloid Interface Sci.* **2020**, *560*, 208−212.
(16) Miraki, M.; Karimi-Maleh, H.; Taher, M. A.; Cheraghi, S.; Karimi, F.; Agarwal, S.; Gupta, V. K. Voltammetric amplified platform based on ionic liquid/NiO nanocomposite for determination of benserazide and levodopa. *J. Mol. Liq.* **2019**, *278*, 672−676.
(17) Prinith, N. S.; Manjunatha, J. G.; Tigari, G.; ALOthman, Z. A.; Alanazi, A. M.; Pandith, A. Mechanistic Insights into the Voltammetric Determination of Riboflavin at Poly (Serine) Modified Graphite and Carbon Nanotube Composite Paste Electrode. *ChemistrySelect* **2021**, *6*, 10746−10757.
(18) Tigari, G.; Manjunatha, J. G.; Raril, C. Electrochemical Determination of Indigotine Based on Poly(Gibberellic Acid)-Modified Carbon Nanotube Paste Electrode. *Environ. Appl. Carbon Nanomater.Based Devices* **2021**, 135−146.
(19) Cross, B. E. Gibberellic acid. Part I. *J. Chem. Soc.* **1954**, 4670.
(20) Prinith, N. S.; Manjunatha, J. G.; Hareesha, N. Electrochemical validation of L-tyrosine with dopamine using composite surfactant modified carbon nanotube electrode. *J. Iran. Chem. Soc.* **2021**, *18*, 3493−3503.
(21) Lin, Q.; Li, Q.; Batchelor-McAuley, C.; Compton, R. G. Two-Electron, Two-Proton Oxidation of Catechol: Kinetics and Apparent Catalysis. *J. Phys. Chem. C* **2015**, *119*, 1489−1495.
(22) Van Maanen, J. M. S.; Verkerk, U. H.; Broersen, J.; Lafleur, M. V. M.; De Vries, J.; Retel, J.; Pinedo, H. M. Semi-Quinone Formation from the Catechol and Ortho-Quinone Metabolites of the Antitumor Agent VP-16−213. *Free Radical Res. Commun.* **1988**, *4*, 371−384.
(23) Shashanka, R.; Jayaprakash, G. K.; Prakashaiah, B.G.; Kumar, M.; Kumara Swamy, B. E. Electrocatalytic determination of ascorbic acid using a green synthesised magnetite nano-flake modified carbon paste electrode by cyclic voltammetric method. *Mater. Res. Innovat.* **2022**, *26*, 229−239.
(24) Rajendrachari, S.; Kumara Swamy, B. E. Biosynthesis of silver nanoparticles using leaves of Acacia melanoxylon and their application as dopamine and hydrogen peroxide sensors. *Phys. Chem. Res.* **2020**, *8*, 1−18.
(25) Jayaprakash, G. K.; Kumara Swamy, B. E.; Rajendrachari, S.; Sharma, S. C.; Flores-Moreno, R. Dual descriptor analysis of cetylpyridinium modified carbon paste electrodes for ascorbic acid sensing applications. *J. Mol. Liq.* **2021**, *334*, 116348.
(26) Shashanka, R.; Chaira, D.; Kumara Swamy, B. E. Electrocatalytic response of duplex and yittria dispersed duplex stainless steel modified carbon paste electrode in detecting folic acid using cyclic voltammetry. *Int. J. Electrochem. Sci.* **2015**, *10*, 5586−5598.
(27) Rajendrachari, S.; Chaira, D.; Kumara Swamy, B. E. Fabrication of yttria dispersed duplex stainless steel electrode to determine dopamine, ascorbic and uric acid electrochemically by using cyclic voltammetry. *Int. J. Sci. Eng. Res.* **2016**, *7*, 1275−1285.
(28) Shashanka, R.; Chaira, D.; Kumara Swamy, B. E. Electrochemical investigation of duplex stainless steel at carbon paste electrode and its application to the detection of dopamine, ascorbic and uric acid. *Int. J. Sci. Eng. Res.* **2015**, *6*, 1863−1871.
(29) Reddy, S.; Kumara Swamy, B. E.; Aruna, S.; Kumar, M.; Shashanka, R.; Jayadevappa, H. Preparation of NiO/ZnO hybrid nanoparticles for electrochemical sensing of dopamine and uric acid. *Chem. Sens.* **2012**, *2*, 7.
(30) Pavitra, V.; Praveen, B. M.; Nagaraju, G.; Shashanka, R. Energy Storage, Photocatalytic and Electrochemical Nitrite Sensing of Ultrasound-Assisted Stable Ta2O5 Nanoparticles. *Top. Catal.* **2022**, DOI: 10.1007/s11244-021-01553-7.
(31) Mahale, R. S.; Shashanka, R.; Vasanth, S.; Vinaykumar, R. Voltammetric Determination of Various Food Azo Dyes Using Different Modified Carbon Paste Electrodes. *Biointerface Res. Appl. Chem.* **2022**, *12*, 4557−4566.
(32) Varun, D. N.; Manjunatha, J. G.; Hareesha, N.; Sandeep, S.; Mallu, P.; Karthik, C. S.; Prinith, N. S.; Sreeharsha, N.; Asdaq, S. M. B. Simple and sensitive electrochemical analysis of riboflavin at functionalized carbon nanofiber modified carbon nanotube sensor. *Monatsh. Chem.* **2021**, *152*, 1183−1191.
(33) Silva, P. S. d.; Gasparini, B. C.; Magosso, H. A.; Spinelli, A. Electrochemical Behavior of Hydroquinone and Catechol at a Silsesquioxane-Modified Carbon Paste Electrode. *J. Braz. Chem. Soc.* **2013**, *24*, 695−699.
(34) Alshahrani, L.; Li, X.; Luo, H.; Yang, L.; Wang, M.; Yan, S.; Liu, P.; Yang, Y.; Li, Q. The Simultaneous Electrochemical Detection of Catechol and Hydroquinone with [Cu(Sal-β-Ala)(3,5-DMPz)2]/SWCNTs/GCE. *Sensors* **2014**, *14*, 22274−22284.
(35) Peng, J.; Gao, Z.-N. Influence of micelles on the electrochemical behaviors of catechol and hydroquinone and their simultaneous determination. *Anal. Bioanal. Chem.* **2006**, *384*, 1525−1532.
(36) Umasankar, Y.; Periasamy, A. P.; Chen, S.-M. Electrocatalysis and simultaneous determination of catechol and quinol by poly-(malachite green) coated multiwalled carbon nanotube film. *Anal. Biochem.* **2011**, *411*, 71−79.
(37) Hu, F.; Chen, S.; Wang, C.; Yuan, R.; Yuan, D.; Wang, C. Study on the application of reduced graphene oxide and multiwall carbon nanotubes hybrid materials for simultaneous determination of catechol, hydroquinone, p-cresol and nitrite. *Anal. Chim. Acta* **2012**, *724*, 40−46.
(38) Si, W.; Lei, W.; Zhang, Y.; Xia, M.; Wang, F.; Hao, Q. Electrodeposition of graphene oxide doped poly(3,4-ethylenedioxythiophene) film and its electrochemical sensing of catechol and hydroquinone. *Electrochim. Acta* **2012**, *85*, 295−301.
(39) Li, M.; Ni, F.; Wang, Y.; Xu, S.; Zhang, D.; Chen, S.; Wang, L. Sensitive and facile determination of catechol and hydroquinone simultaneously under coexistence of resorcinol with a Zn/Al layered double hydroxide film modified glassy carbon electrode. *Electroanalysis* **2009**, *21*, 1521−1526.
(40) Caballero, S. J.; Guerrero, M. A.; Vargas, L. Y.; Ortiz, C. C.; Castillo, J. J.; Gutiérrez, J. A.; Blanco, S. Electroanalytical determination of catechol by a biosensor based on laccase from Aspergillus oryzae immobilized on gold screen-printed electrodes. *J. Phys.: Conf. Ser.* **2018**, *1119*, 012009.

https://doi.org/10.1021/acsomega.2c02553
ACS Omega 2022, 7, 24679−24687

(41) Zhao, D.-M.; Zhang, X.-H.; Feng, L.-J.; Jia, L.; Wang, S.-F. Simultaneous determination of hydroquinone and catechol at PASA/MWNTs composite film modified glassy carbon electrode. *Colloids Surf., B* **2009**, *74*, 317−321.
(42) Manjunatha, J. G. Electrochemical Polymerised Graphene Paste Electrode and Application to Catechol Sensing. *Open Chem. Eng. J.* **2019**, *13*, 81−87.
(43) Manjunatha, J. G. Fabrication of Efficient and Selective Modified Graphene Paste Sensor for the Determination of Catechol and Hydroquinone. *Surfaces* **2020**, *3*, 473−483.
(44) Chen, Y.; Liu, X.; Zhang, S.; Yang, L.; Liu, M.; Zhang, Y.; Yao, S. Ultrasensitive and simultaneous detection of hydroquinone, catechol and resorcinol based on the electrochemical co-reduction prepared Au-Pd nanoflower/reduced graphene oxide nanocomposite. *Electrochim. Acta* **2017**, *231*, 677−685.
(45) Lai, T.; Cai, W.; Dai, W.; Ye, J. Easy processing laser reduced graphene: A green and fast sensing platform for hydroquinone and catechol simultaneous determination. *Electrochim. Acta* **2014**, *138*, 48−55.
(46) Li, S.-J.; Qian, C.; Wang, K.; Hua, B.-Y.; Wang, F.-B.; Sheng, Z.-H.; Xia, X.-H. Application of thermally reduced graphene oxide modified electrode in simultaneous determination of dihydroxybenzene isomers. *Sens. Actuators, B* **2012**, *174*, 441−448.
(47) Ma, L.; Zhao, G.-C. Simultaneous Determination of Hydroquinone, Catechol and Resorcinol at Graphene Doped Carbon Ionic Liquid Electrode. *Int. J. Electrochem.* **2012**, *2012*, 243031.
(48) Wang, L.; Huang, P.; Bai, J.; Wang, H.; Zhang, L.; Zhao, Y. Simultaneous electrochemical determination of phenol isomers in binary mixtures at a poly(phenyalanine) modified glassy carbon electrode. *Int. J. Electrochem. Sci.* **2006**, *1*, 403−413.
(49) Zhu, M.; Xu, R.; Wang, X.; Zhang, J. L. Q.; Wei, J. MIL-101 (Fe) modified carbon paste electrode for the efficient simultaneous detection of hydroquinone and catechol. *Int. J. Electrochem. Sci.* **2021**, *16*, 211228.
(50) Ding, Y.-P.; Liu, W.-L.; Wu, Q.-S.; Wang, X.-G. Direct simultaneous determination of dihydroxybenzene isomers at C-nanotube-modified electrodes by derivative voltammetry. *J. Electroanal. Chem.* **2005**, *575*, 275−280.

https://doi.org/10.1021/acsomega.2c02553
ACS Omega 2022, 7, 24679−24687